Sonja Kleffel,[1] Andrea Vergani,[1,2] Sara Tezza,[1] Moufida Ben Nasr,[1] Monika A. Niewczas,[3] Susan Wong,[4] Roberto Bassi,[1] Francesca D'Addio,[1,2] Tobias Schatton,[5,6] Reza Abdi,[7] Mark Atkinson,[8] Mohamed H. Sayegh,[6] Li Wen,[9] Clive H. Wasserfall,[8] Kevin C. O'Connor,[10] and Paolo Fiorina[1,2]

Interleukin-10$^+$ Regulatory B Cells Arise Within Antigen-Experienced CD40$^+$ B Cells to Maintain Tolerance to Islet Autoantigens

Diabetes 2015;64:158–171 | DOI: 10.2337/db13-1639

Impaired regulatory B cell (Breg) responses are associated with several autoimmune diseases in humans; however, the role of Bregs in type 1 diabetes (T1D) remains unclear. We hypothesized that naturally occurring, interleukin-10 (IL-10)–producing Bregs maintain tolerance to islet autoantigens, and that hyperglycemic nonobese diabetic (NOD) mice and T1D patients lack these potent negative regulators. IgV_H transcriptome analysis revealed that islet-infiltrating B cells in long-term normoglycemic (Lnglc) NOD, which are naturally protected from diabetes, are more antigen-experienced and possess more diverse B-cell receptor repertoires compared to those of hyperglycemic (Hglc) mice. Importantly, increased levels of Breg-promoting CD40$^+$ B cells and IL-10–producing B cells were found within islets of Lnglc compared to Hglc NOD. Likewise, healthy individuals showed increased frequencies of both CD40$^+$ and IL-10$^+$ B cells compared to T1D patients. Rituximab-mediated B-cell depletion followed by adoptive transfer of B cells from Hglc mice induced hyperglycemia in Lnglc human CD20 transgenic NOD mouse models. Importantly, both murine and human IL-10$^+$ B cells significantly abrogated T-cell–mediated responses to self- or islet-specific peptides ex vivo. Together, our data suggest that antigen-matured Bregs may maintain tolerance to islet autoantigens by selectively suppressing autoreactive T-cell responses, and that Hglc mice and individuals with T1D lack this population of Bregs.

Although type 1 diabetes (T1D) has been classically described as a CD4$^+$ T-cell–mediated disease, B cells play a crucial role in the autoimmune destruction of pancreatic islets (1–4). B cells can promote T1D by *1*) presenting islet-derived peptides to autoreactive T cells (2,4–10), *2*) producing autoantibodies (aAbs) against β-cell antigens (Ags) (7,11,12), and *3*) secreting proinflammatory cytokines (2,3,13,14). B-cell depletion in nonobese diabetic (NOD) mice as well as neutralization of the B-cell–activating factor (BAFF) delay the onset of diabetes in prediabetic NOD mice and re-establishes normoglycemia in hyperglycemic NOD mice (3,15–18). Likewise, B-cell depletion in individuals newly diagnosed with T1D prevents decline of the islet

[1]Nephrology Division, Boston Children's Hospital, Harvard Medical School, Boston, MA
[2]Transplant Medicine, Istituto di Ricovero e Cura a Carattere Scientifico Ospedale San Raffaele, Milano, Italy
[3]Section on Genetics and Epidemiology, Research Division, Joslin Diabetes Center and Department of Medicine, Harvard Medical School, Boston, MA
[4]Institute of Molecular and Experimental Medicine, Cardiff University School of Medicine, Cardiff, U.K.
[5]Harvard Skin Disease Research Center, Department of Dermatology, Brigham and Women's Hospital, Harvard Medical School, Boston, MA
[6]Transplant Research Program, Boston Children's Hospital, Harvard Medical School, Boston, MA
[7]Nephrology Division, Brigham and Women's Hospital, Harvard Medical School, Boston, MA
[8]Department of Pathology, Immunology and Laboratory Medicine, University of Florida, Gainesville, FL
[9]Department of Immunology, Yale School of Medicine, New Haven, CT
[10]Department of Neurology, Yale School of Medicine, New Haven, CT
Corresponding author: Paolo Fiorina, paolo.fiorina@childrens.harvard.edu.

Received 23 October 2013 and accepted 31 July 2014.
This article contains Supplementary Data online at http://diabetes.diabetesjournals.org/lookup/suppl/doi:10.2337/db13-1639/-/DC1.
S.K. and A.V. contributed equally to this work.

mass (19). Importantly, preclinical and clinical studies suggest that re-emerging B cells exhibit an immunosuppressive phenotype that may directly contribute to the clinical efficacy of B-cell depletion therapies (3,15,20). Recent evidence supports the existence of regulatory B cells (Bregs), which, like regulatory T cells (Tregs), are able to negatively modulate T-cell–dependent autoimmune responses in an Ag-specific manner (14,21–28). To date, several populations of murine and human Bregs have been described based on the expression of various surface markers. Reported phenotypes for murine Bregs include $CD19^+CD1d^{hi}CD5^+$ (26,27,29), $CD19^+CD21^{hi}IgM^{hi}CD23^{hi}$ (30–32), and $CD19^+$Tim-1^+ (33). Human Breg populations have been identified based on expression of $CD19^+CD27^-CD24^{hi}CD38^{hi}$ (immature Bregs) (34) or $CD19^+CD27^+CD24^{hi}$ (memory B cells) (21) surface markers. Lineage-specific markers to exclusively identify Breg populations have yet to be described. The expression of the cytokine interleukin-10 (IL-10) appears to be the only known distinguishing feature and the central mediator that conveys the immunosuppressive functions of all Bregs subsets (24,28,35,36). Bregs have been previously shown to suppress autoimmune disease in mouse models of experimental autoimmune encephalomyelitis (EAE) (23,37) and arthritis (31), and impaired Breg responses are associated with several autoimmune diseases in humans, including multiple sclerosis (38) and lupus erythematosus (34). However, the role of Bregs in autoimmune T1D remains unknown. Moreover, the mechanisms regulating *1*) the selective inhibition of antigen-specific immune responses and *2*) the physiological signals controlling IL-10 production by Bregs require further elucidation.

Although reports indicate that ~20% of NOD mice are naturally protected against the spontaneous development of diabetes (39), the mechanisms underlying this protection have yet to be identified (40). We previously showed that following depletion of the B-cell pool in NOD mice, the re-emerging B cells exhibit an immunosuppressive phenotype and inhibited diabetes onset (3). Furthermore, published data from other groups suggest a key role for Bregs in limiting autoimmune disease. On this basis, we hypothesized that *1*) a population of naturally occurring, islet-infiltrating Bregs abrogates autoimmune responses and thus protects these 20% of NOD mice from the onset of autoimmune diabetes and *2*) hyperglycemic NOD mice and individuals with T1D lack this population of Bregs.

RESEARCH DESIGN AND METHODS

Patient Characteristics

Blood samples were obtained from healthy individuals and from individuals with T1D and their first-degree relatives who were free from diabetes but had detectable levels of the aAbs anti-GAD and anti–IA-2 in their peripheral blood (Table 1), in accordance with the Joslin Diabetes Center and Boston Children's Hospital Institutional Review Boards.

Animals

Female NOD/ShiLtJ (NOD), NOD.CB17-Prkdcscid/J (NOD.Scid), NOR/LtJ, NOD.BDC2.5 (BDC2.5), and C57BL/6J (B6) mice were purchased from The Jackson Laboratory (Bar Harbor, ME). Human CD20 transgenic NOD mice [hCD20($^{+/+}$) NOD] were generated and maintained as previously reported (15). All mice were used according to institutional guidelines, and animal protocols were approved by the Boston Children's Hospital Institutional Animal Care and Use Committee.

Table 1—Characteristics of healthy individuals, aAb^+ relatives of T1D patients who are free from disease, and individuals with T1D

	Healthy individuals (n = 10)	aAb^+ relatives (n = 8)	Individuals with T1D (n = 25)
Sex (n)			
Male	7	4	13
Female	3	4	12
Age, mean ± SEM (years)	32.1 ± 2.2	26.3 ± 5.3	53.2 ± 2.3
T1D, mean ± SEM (years)	—	—	35.0 ± 2.4
GAD aAb^+ (>18 IU/mL) (n)	0	7	25
IA-2 aAb^+ (>15 IU/mL) (n)	0	5	25

Diabetes Monitoring and Insulitis Scoring

Overt diabetes was defined as blood glucose levels above 250 mg/dL for 3 consecutive days. Blood glucose was measured using the OneTouch Ultra (LifeScan Inc., Milpitas, CA) blood glucose meter. Insulitis score was determined on 150 hematoxylin and eosin (H&E)-stained islets per group (n = 3 mice), as previously described (41).

Murine Ex Vivo Breg Suppression Assay

Splenic $CD4^+$ T cells (2×10^5) were isolated from BDC2.5 TCR transgenic mice using $CD4^+$ monoclonal (m)Ab-coated microbeads (Miltenyi Biotec, Bergisch Gladbach, Germany) stimulated with 150 ng/mL BDC2.5 peptide and cocultured with splenic IL-10–producing B cells isolated from NOD mice using the Breg isolation kit (Miltenyi Biotec) in a 2:1 ratio, respectively. When indicated, dendritic cells (DCs), isolated using $CD11c^+$ mAb-coated microbeads (Miltenyi Biotec), were added in a 2:1:1 ratio as described (42,43). To study the effect of IL-10 secreted by $IL\text{-}10^+$ Bregs on T-effector cell activation and differentiation, 5 μg/mL of anti–IL-10 blocking Ab was added to the coculture system. Interferon-γ (IFN-γ) ELISA spot (ELISPOT) assays and flow cytometric analysis of cytokine production and activation marker expression were performed as described.

Human Ex Vivo Breg Generation

B cells were isolated from lymphocyte preparations of peripheral blood mononuclear cells (PBMCs) of healthy donors, T1D individuals, and their aAb^+, diabetes-free relatives using CD19 mAb-coated microbeads (Miltenyi Biotec). B cells (2.5×10^5) were cultured for 4 days in the presence of anti-human CD40 ligand (2 μg/mL; R&D

Systems) and lipopolysaccharide (10 μg/mL; Sigma-Aldrich, St. Louis, MO) in RPMI-1640 (Gibco, Grand Island, NY) containing 10% human serum (Mediatech Inc., Herndon, VA).

Statistical Analysis

Unless otherwise indicated, all data are shown as mean ± SEM. Statistical analysis was performed using the unpaired Student *t* test. A two-sided value of $P \leq 0.05$ was considered statistically significant. The Kaplan-Meier curve with the Wilcoxon test was used to analyze the development of diabetes in mice. Statistical analysis was performed using GraphPad Prism software (GraphPad Software, Inc., La Jolla, CA).

RESULTS

Islets of Long-term Normoglycemic NOD Mice Exhibit a Reduced Lymphoid Infiltrate

To study B-cell infiltration patterns of pancreatic islets during the onset and progression of T1D in NOD mice, histological grading was performed on pancreatic cross-sections of 4- and 10-week-old normoglycemic (Nglc), hyperglycemic (Hglc) (average age, 19 weeks), and long-term normoglycemic (Lnglc) (average age, 30 weeks) female NOD, as well as 10-week-old nonautoimmune B6 mice.

Islets of 4-week-old Nglc NOD mice and B6 nonautoimmune control mice demonstrated a well-preserved islet architecture with abundant insulin staining devoid of lymphoid infiltrate as indicated by negative staining for the pan–B-cell marker B220 and the T-cell marker CD3 (Fig. 1*A* and *B*). Islets from 10-week-old Nglc and Lnglc NOD mice exhibited peri-insulitis, constituted by B cells and T cells (Fig. 1*A* and *B*). Insulin staining was preserved despite infiltration (Fig. 1*B*). Conversely, islets from Hglc NOD mice exhibited substantial lymphoid infiltrate, consisting of clustered $B220^+$ B cells and scattered $CD3^+$ T cells, while staining negative for insulin. Overall, islets from Lnglc mice showed a reduced, less organized B-cell–infiltration pattern when compared with Hglc NOD mice. Consistent with histopathological findings, islet-specific B220 mRNA expression was upregulated 13.4-fold in 10-week-old Nglc NOD mice ($P \leq 0.05$), 23.7-fold in Hglc mice ($P \leq 0.05$), and 20.5-fold in Lnglc NOD mice compared with 4-week-old mice ($P \leq 0.001$), as determined by quantitative real-time PCR (Fig. 1*C*).

To address whether differences in the humoral immune response may convey protection against the autoimmune destruction of pancreatic islets in Lnglc NOD mice, we analyzed serum insulin aAb (IAA) (Fig. 1*D*) levels in different groups of NOD mice; however, no significant differences were observed. BAFF (Fig. 1*E*) was significantly ($P \leq 0.05$) elevated in the serum of 10-week-old Nglc, Hglc, and Lnglc NOD when compared to 4-week-old mice.

Increased Levels of Apoptotic Islet-Infiltrating B Cells and a Reduction in Germinal Center–like Structures Are Evident in Lnglc NOD Mice

Serial pancreatic tissue sections were stained for the pan–B-cell marker B220, the proliferation marker Ki-67, and TUNEL assay to assess a potential imbalance between proliferating and apoptotic B cells. No significant differences were evident in B-cell proliferation or apoptosis among Hglc and Lnglc NOD mice (Fig. 1*F*). Importantly, a significant ($P \leq 0.001$) increase in apoptotic B cells was detected within islet-infiltrating B-cell populations of Lnglc, but not Hglc, compared with 10-week-old Nglc NOD mice (Fig. 1*F*). Because mice are not fully grown until 8 weeks of age, the pancreatic tissue of 4-week-old NOD mice showed Ki-67 positivity (Fig. 1*B*, panel 26).

Ectopic germinal center (GC)–like structures were quantified based on simultaneous expression of Bcl-6, Ki-67, and PNA-binding sites within morphologically distinct areas of proliferating $B220^+$ B cells on serial tissue sections (Fig. 1*H* shows an examplary case from a 10-week-old NOD mouse). No ectopic GCs were identified in pancreatic islets of 4-week-old Nglc NOD or B6 control mice; however, 2.0% of islets of 10-week-old Nglc and Hglc NOD mice ($P \leq 0.001$ vs. 4-week-old Nglc NOD, respectively) and 1.3% of islets of Lnglc mice (NS) contained extranodal GCs (Fig. 1*G*).

Islet-Infiltrating B Cells From Lnglc NOD Mice Show Elevated Mutation Frequencies Within B-Cell Receptor Transcripts

To characterize the islet-infiltrating B-cell repertoire in the different groups of NOD mice, B-cell receptor sequence libraries were generated (44,45) from individual islets, and the variable region of the heavy chain (V_H) was analyzed. A comparison of immunoglobulin (Ig)V_H sequences from the islet-infiltrating B-cell repertoire of NOD mice to germline segments using IMGT/V-QUEST software revealed both silent and amino acid replacement mutations throughout the variable regions of the B-cell receptor. Compared with the germline, low frequencies of nucleotide mutations per IgV_H transcript were found in 4- and 10-week-old Nglc NOD mice, indicating a primarily naïve B-cell phenotype (Fig. 2*A* and *B*). No significant increases in the number of nucleotide mutations were observed in B-cell receptor libraries of Hglc NOD mice; however, the islet-infiltrating B-cell repertoire of Lnglc mice showed significantly higher mutation rates compared with 10-week-old Nglc NOD mice ($P \leq 0.05$) (Fig. 2*A* and *B*). Similarly, islet-infiltrating B cells from 4- and 10-week-old Nglc NOD mice acquired less than two amino acid replacement mutations per transcript within the IgV_H region (NS) (Fig. 2*C* and *D*). However, significant increases in amino acid replacement mutations were evident in Lnglc, but not Hglc, NOD mice compared with 4-week-old Nglc and with 10-week-old Nglc mice ($P \leq 0.05$, respectively) (Fig. 2*C* and *D*).

Islet-Infiltrating B Cells From Lnglc NOD Mice Exhibit a Broader Isotype Expression

The complementarity-determining region 3 (CDR3) within the variable region of the IgV_H plays an important role in determining Ag specificity by forming part of the epitope-binding site. Nucleotide and amino acid mutations within

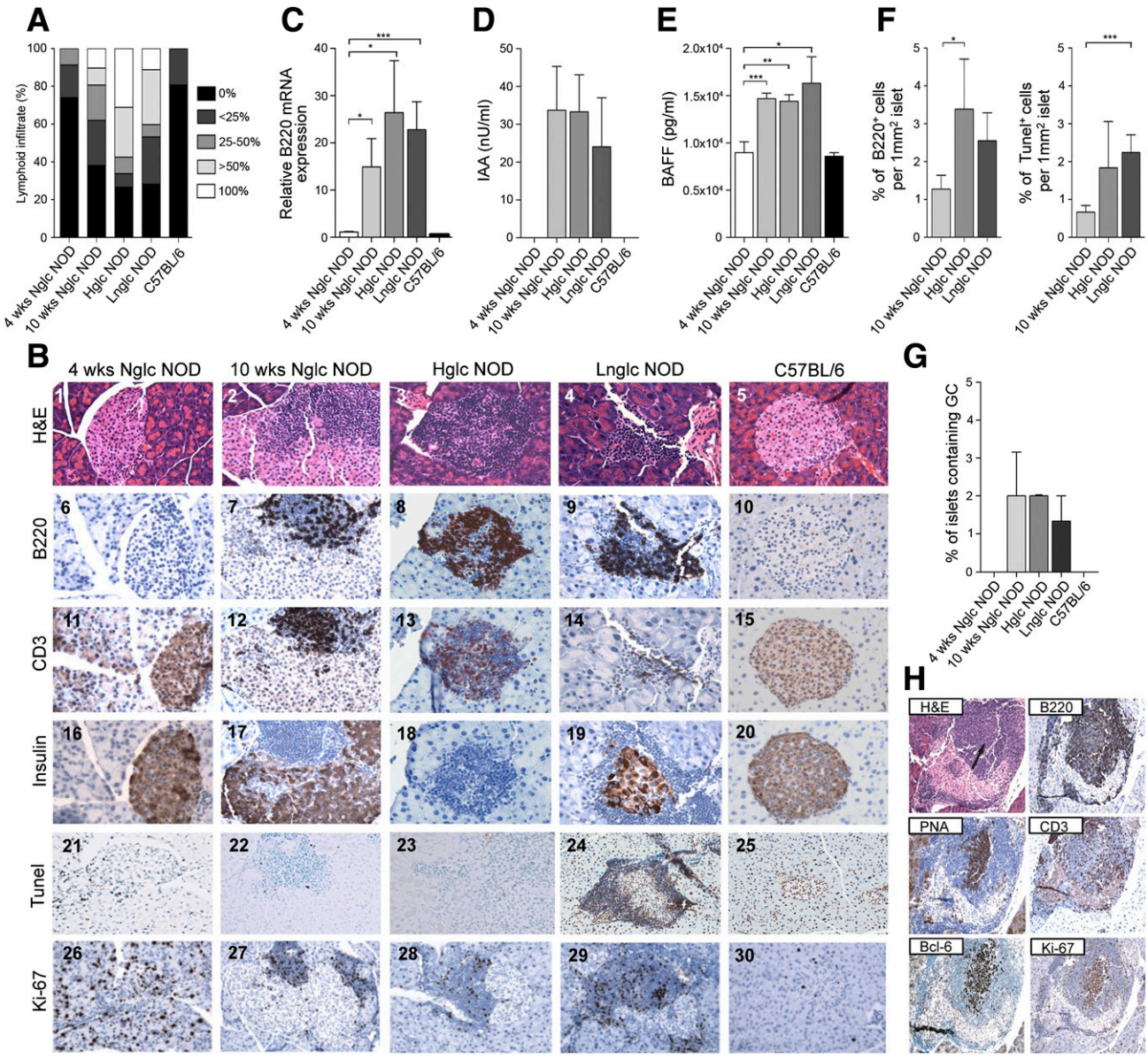

Figure 1—Characterization of pancreatic islets in NOD mice. *A*: Quantification of lymphoid infiltrate by insulitis scoring of H&E–stained pancreatic tissue sections. *B*: Representative H&E staining (1–5) and immunohistochemical (IHC) analysis of B220 (6–10), CD3 (11–15), insulin (16–20), TUNEL (21–25), and Ki-67 (26–30) expression in serial pancreatic islet tissue sections from NOD mice. *C*: Relative B220 mRNA expression within the pancreatic islet as determined by quantitative PCR amplification. *D*: Serum levels of IAA and (*E*) BAFF, as determined by radioassay analysis. *F*: Computer-aided quantification of B220 expression and TUNEL positivity of IHC-stained pancreatic tissue sections. *G*: Quantification of ectopic GCs in IHC-stained serial pancreatic tissue sections for B220, Bcl-6, PNA, CD3, and Ki-67. *H*: Representative IHC images of an ectopic GC within the pancreatic islets of a 10-week-old Nglc NOD mouse. Bars represent mean ± SEM. wks, weeks. $^{*}P \leq 0.05$; $^{**}P \leq 0.01$; $^{***}P \leq 0.001$.

the CDR3 region were detected in B cells isolated from individual islets of all groups of NOD mice. No significant differences in frequencies of amino acid mutations within the CDR3 region were observed in 4-week-old Nglc, 10-week-old Nglc, Hglc, and Lnglc mice (Fig. 2*E* and *F*, NS). A semi-nested PCR approach was used to amplify IgV_H genes from islet-harbored B cells to study isotype expression among the B-cell infiltrate. The diversity of different isotypes expressed by the B-cell infiltrate was determined from sequence analysis of the isotype-specific constant regions and visualized by agarose gel separation of isotype-specific PCR products. Amplification of the IgV_H gene repertoire of B cells isolated from cross-sections of individual islets of 4-week-old Nglc NOD mice showed that 100% of the islets examined were infiltrated with B cells expressing IgM, whereas only 20% of the islets were infiltrated with detectable levels of B cells expressing IgG1, IgG2a/c, and IgG2b. No detectable levels of B cells expressing IgG3 were isolated from islets of 4-week-old Nglc NOD mice (Fig. 3*A*). Similarly, 100% of islets isolated

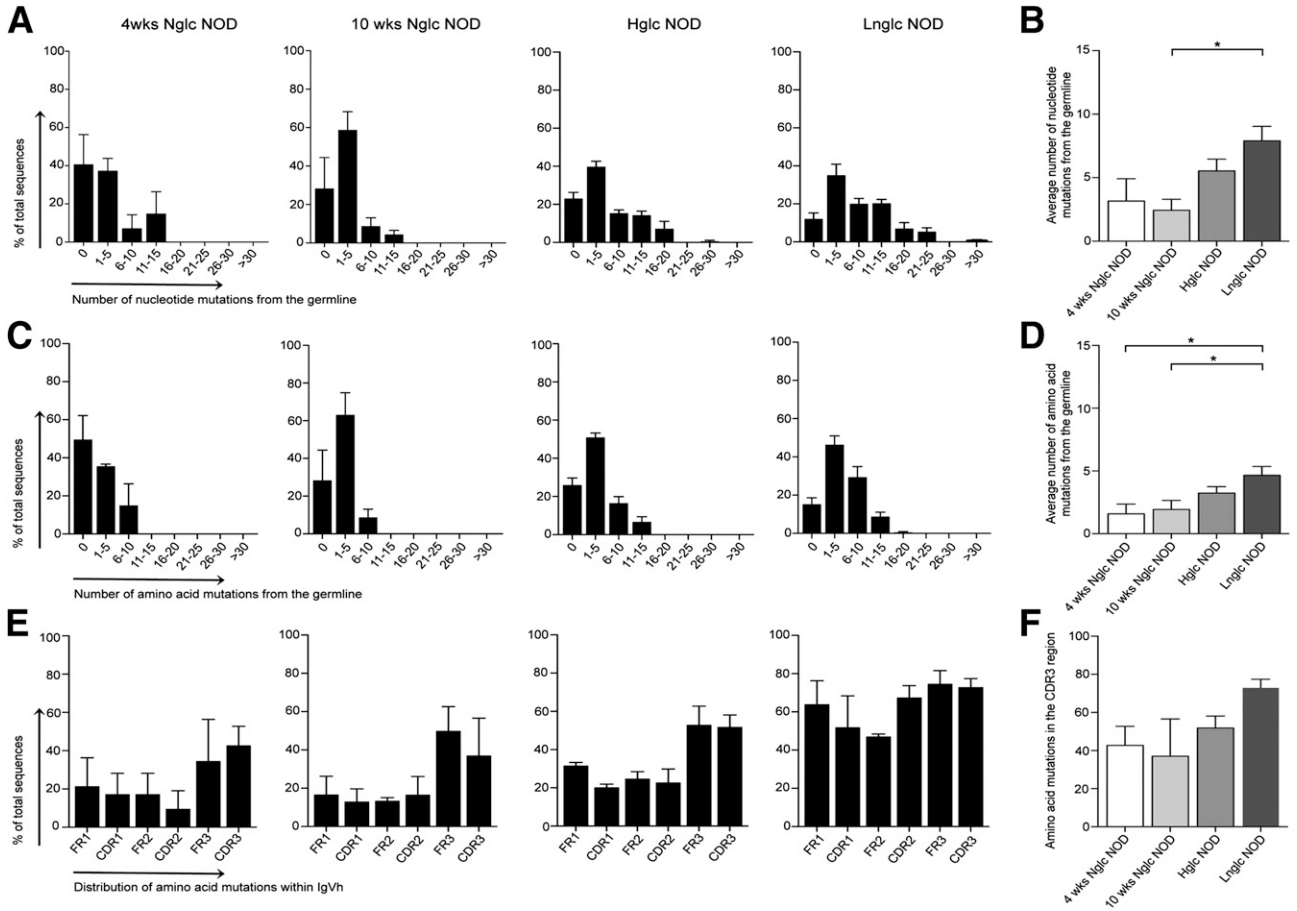

Figure 2—IgV_H transcriptome analysis of islet-infiltrating B cells isolated from different groups of NOD mice. (*A*) Quantification of nucleotide mutations from the germline within the entire IgV_H sequence and (*B*) summary of the average number of nucleotide mutations per group. (*C*) Quantification of amino acid replacement mutations from the germline within the entire IgV_H sequences and (*D*) summary of the average number of amino acid mutations per group. (*E*) Distribution of amino acid mutations within the framework (FR) and the CDR of the IgV_H region and (*F*) the average numbers of amino acid mutations within the CDR3 region. Bars represent mean ± SEM. wks, weeks. $^*P \leq 0.05$.

from 10-week-old Nglc NOD mice were infiltrated by B cells expressing IgM and IgG2a/c, whereas IgG1 expressing B cells were found in 60% of islets and $IgG2b^+$ expressing B cells were found in 20% of islets. No B cells expressing IgG3 were found infiltrating the islets of these mice (Fig. 3*A*). Taken together, the isotype profile of islet-infiltrating B cells suggests a naïve B-cell pool present in islets isolated from 4- and 10-week-old Nglc NOD mice. In contrast, most of the islet-infiltrating B cells from Hglc and Lnglc NOD mice had class switched from IgM to IgG isotypes (IgG1: 83 and 71%; IgG2a/c: 100 and 60%; IgG2b: 100 and 81%; IgG3: 83 and 57% in Hglc and Lnglc mice, respectively), demonstrating an Ag-experienced phenotype for most of the B cells (Fig. 3*A*). Representative agarose gel images visualizing isotype distribution within individual islets for each group are shown in Fig. 3*B*.

Islet-Infiltrating B Cells From Lnglc NOD Mice Are Clonally Expanded

In addition to somatic hypermutation and class switching, IgV_H sequences within libraries constructed from pancreatic islets of different groups of NOD mice were analyzed for evidence of clonal expansion. Sequences were considered progeny of the same clone when their CDR3 region was identical and the IgV_H did not differ in more than one nucleotide replacement mutation. Analysis of IgV_H sequence libraries constructed from 4- and 10-week-old Nglc and Hglc NOD mice showed that the number of clones per 100 sequences analyzed corresponded with disease progression (Fig. 3*C*). Interestingly, fewer individual clones where found within libraries constructed from islet cross-sections of Lnglc compared with Hglc NOD mice (NS) (Fig. 3*C*). The CDR3 sequences of the individual clones within B-cell receptor libraries can be found in the Supplementary Table 1.

Next, we screened for clonal variants to determine whether diversification of variable regions in B cells had yielded a mature B-cell receptor repertoire. We defined IgV_H sequences as clonally related variants when they shared recombination events in the VDJ junction, as indicated by identical CDR3 regions, and differed in at least two nucleotide replacement mutations. Sequence analysis

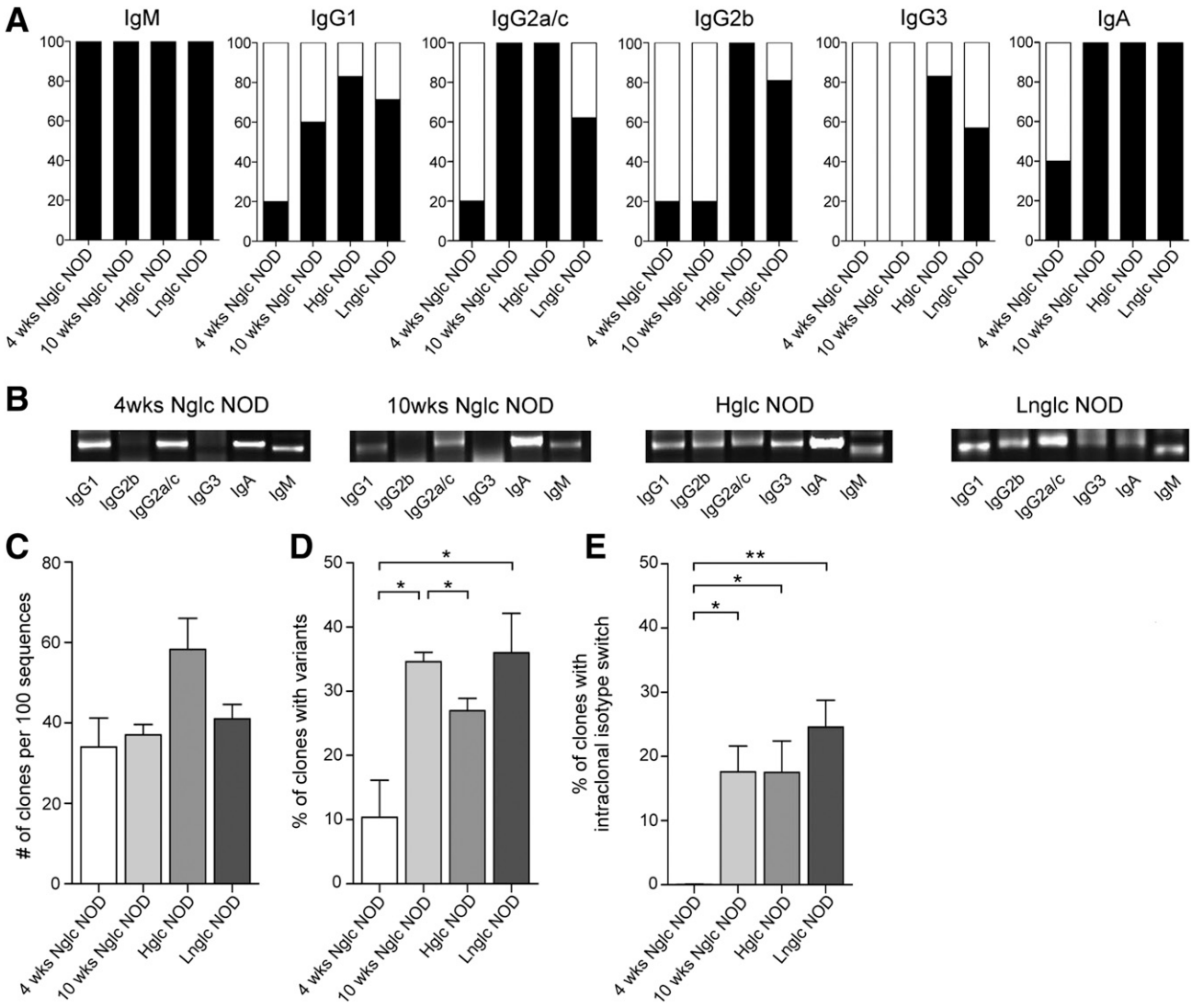

Figure 3—Molecular characterization of islet-infiltrating B cells obtained from different groups of NOD mice. *A*: Isotype-specific mRNA expression as determined by RT-PCR amplification and sequencing of isotype-specific Ig constant region domains of islet-infiltrating B cells. *B*: Representative agarose gel images. *C*: Quantification of B-cell clones within B-cell receptor libraries by analysis of their unique CDR3 sequences. *D*: Assessment of clonal variants by analysis of IgV_H regions within clonal populations with identical CDR3 sequences. *E*: Quantification of intraclonal isotype switches as determined by isotype-specific constant region analysis of sequences with identical CDR3 regions. Bars represent means ± SEM. wks, weeks. $^*P \leq 0.05$; $^{**}P \leq 0.01$.

revealed significantly ($P \leq 0.05$) higher percentages of clones with variants in 10-week-old Nglc and Lnglc compared with 4-week-old Nglc NOD mice (Fig. 3*D*). Intraclonal isotype switches were not observed in B-cell receptor libraries obtained from 4-week-old Nglc NOD mice; however, libraries generated from 10-week-old Nglc, Hglc, and, to an even greater extent, Lnglc demonstrated markedly enhanced ($P \leq 0.05$) frequencies of intraclonal isotype switches (Fig. 3*E*).

Islet-Infiltrating B Cells From Lnglc NOD Mice Exhibit Increased Frequencies of CD40$^+$, Anergic, and IL-10$^+$ B Cells

CD40 ligation is known to play a key role in B-cell proliferation, induction of Ig class switches, somatic hypermutation, and generation of Bregs (24). Although the frequencies of splenic B220$^+$ B cells expressing CD40 (Fig. 4*A*), CD80 (Fig. 4*C*), and MHC class II (Fig. 4*E*) isolated from B6, NOR, 10-week-old Nglc, Hglc, and Lnglc NOD mice were not statistically different, significantly higher percentages of splenic B cells expressing both CD40 and MHC class II were observed in 4-week-old Nglc NOD mice compared with the other groups ($P \leq 0.05$) (Fig. 4*A* and *E*). Interestingly, the frequency of islet-infiltrating B cells expressing CD40 (Fig. 4*B*), but not CD80 and MHC class II (Fig. 4*D* and *F*), was significantly ($P \leq 0.05$) increased in Lnglc compared with 10-week-old Nglc but not Hglc NOD mice. The percentages of B220$^+$CD93$^+$CD23$^+$IgM^{low} anergic B cells (46) obtained from splenocytes were similar between the

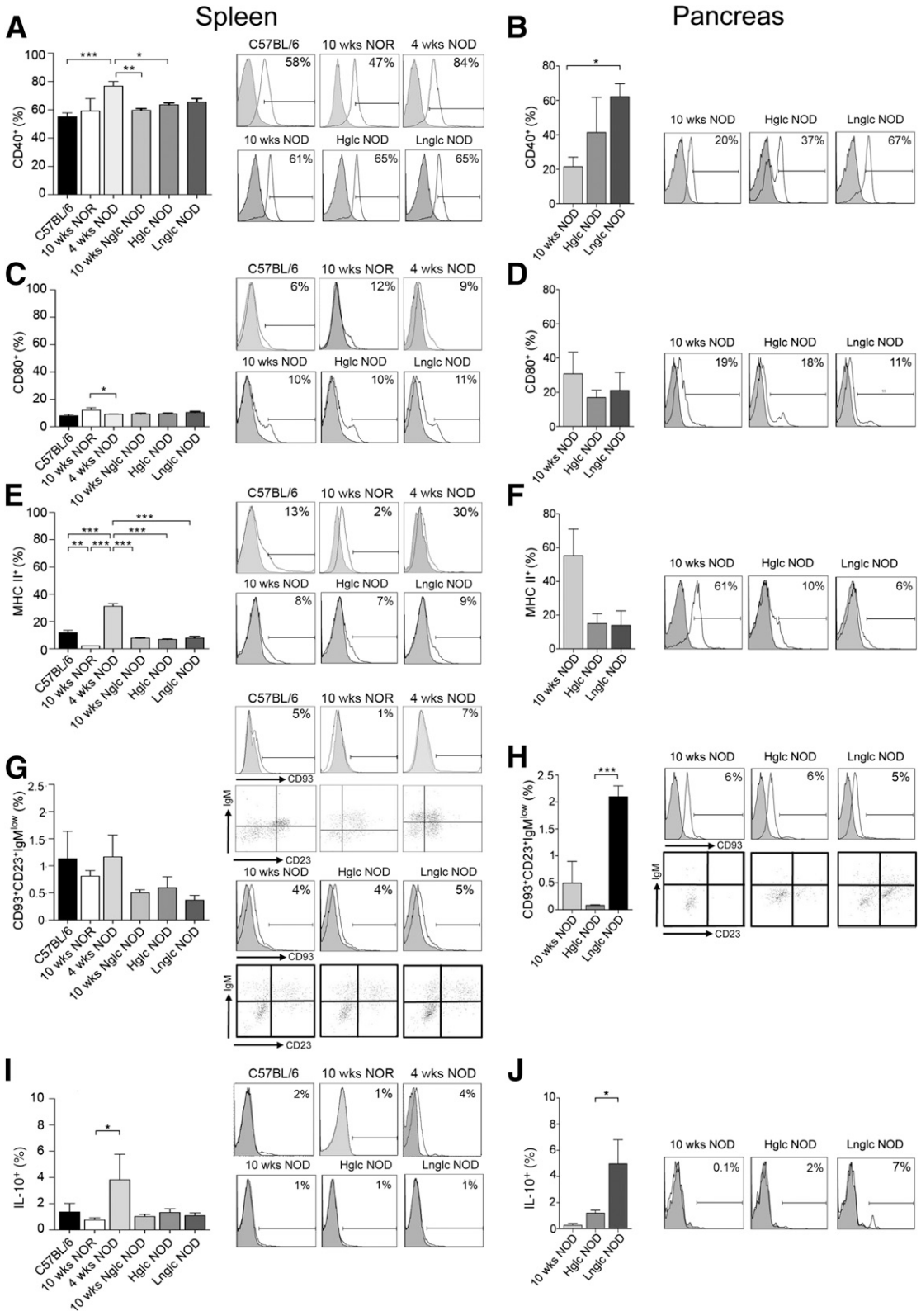

Figure 4—Phenotypic characterization of splenic and pancreatic murine B cells isolated from C57BL/6, NOR, and NOD mice, as indicated. Flow cytometric analysis for expression of CD40 by splenic (*A*) or pancreatic (*B*) $B220^+$ B cells, CD80 by splenic (*C*) or pancreatic (*D*) $B220^+$ B cells, and MHC II by splenic (*E*) or pancreatic (*F*) $B220^+$ B cells. Assessment of anergic $CD93^+CD23^+IgM^{low}$ splenic (*G*) or pancreatic $B220^+$ (*H*) B cells, as determined by flow cytometry. IL-10 expression by splenic (*I*) vs. pancreatic (*J*) $B220^+$ B cells as determined by intracellular flow cytometric staining. White peaks indicate antigen-specific staining, gray peaks show respective isotype control staining. Mean percentages ± SEM of marker expression (left) and representative flow cytometry plots (right), respectively. wks, weeks. $^*P \leq 0.05$; $^{**}P \leq 0.01$; $^{***}P \leq 0.001$.

different groups (Fig. 4*G*). Frequencies of anergic B cells in islets of 10-week-old Nglc and Hglc NOD mice were comparable to those observed in the spleen; however, a significant ($P \leq 0.001$) increase in the percentage of islet-infiltrating anergic B cells was observed in Lnglc NOD mice (Fig. 4*H*). Finally, the frequencies of naturally occurring IL-10$^+$ B cells, suggested to be endowed with immunoregulatory properties (14,22,26), were then analyzed. Percentages of IL-10$^+$ B cells recovered from the spleens of B6, 10-week-old NOR, 4-week-old Nglc, and 10-week-old Nglc, Hglc, or Lnglc NOD mice were similar among groups (NS) (Fig. 4*I*). The frequencies of IL-10$^+$ B cells among the islet-infiltrating B-cell pool of 10-week-old Nglc and Hglc NOD mice were comparable to frequencies observed in the spleen; however, the percentages of islet-infiltrating IL-10$^+$ B cells isolated from the pancreata of Lnglc NOD mice were significantly higher ($P \leq 0.05$) (Fig. 4*J*). Importantly, frequencies of CD4$^+$CD25$^+$FoxP3$^+$ Tregs were not significantly different among islet-infiltrating lymphocytes obtained from Hglc and Lnglc NOD mice (data not shown).

Peripheral B Cells From NOD Mice Lack Regulatory Properties Ex Vivo

To assess the ability of total splenic B-cell populations to present BDC2.5 peptides and hence to stimulate autoreactive BDC2.5 transgenic CD4$^+$ T cells, IFN-γ production by responder T cells was measured. Total splenic B cells isolated from 10-week-old Nglc NOD mice stimulated autoreactive CD4$^+$ T cells more efficiently ($P \leq 0.05$) than B-cell populations isolated from Hglc or Lnglc NOD mice, respectively (Fig. 5*A*). Next, we assessed whether total splenic B cells were endowed with immunoregulatory properties. Although the addition of B cells from the three experimental groups augmented T-cell activation compared with cocultures of CD4$^+$ T cells with CD11c$^+$ DC alone, no significant differences in IFN-γ production were evident in cocultures with B cells from 10-week-old Nglc, Hglc, and Lnglc NOD mice (Fig. 5*B*), suggesting that peripheral B-cell populations have stimulatory but not regulatory properties.

Peripheral B Cells From NOD Mice Lack Regulatory Properties In Vivo

To evaluate the regulatory properties of peripheral B cells from 10-week-old Nglc, Hglc, and Lnglc NOD mice in vivo, B220$^+$ B-cell and CD4$^+$ T-cell populations were isolated from the different groups of NOD mice and adoptively transferred into NOD.Scid mice (n = 5, respectively). No significant differences in diabetes onset were observed among mice injected with B and T cells from Hglc mice, B cells from 10-week-old Nglc and T cells from Hglc mice, B cells from Lnglc and T cells from Hglc mice, or mice injected with T cells from Hglc mice alone (Fig. 5*C*). Interestingly, all NOD.Scid recipient mice that received CD4$^+$ T cells from Lnglc mice remained normoglycemic after a 20-week follow-up (Fig. 5*C*).

IL-10$^+$ B Cells From Nglc NOD Mice Exhibit Decreased Ag-Presenting Functions Ex Vivo

To study whether IL-10–producing B-cell subsets exhibit deficits in Ag presentation, B220$^+$ cells producing IL-10 versus IL-10$^-$ B-cell bulk populations were isolated from the spleen of Nglc NOD mice and cocultured with BDC2.5 transgenic CD4$^+$ T cells in the presence of BDC2.5 peptide. Upon isolation, IL-10–producing B220$^+$ cells (IL-10$^+$ B cells) were enriched by >12-fold compared to the flow-through B-cell subset (IL-10$^-$ B cells) (Fig. 5*D*). Interestingly, compared IL-10$^-$ B-cell populations, cocultures with IL-10$^+$ B cells resulted in significantly reduced ($P \leq 0.05$) levels of IFN-γ production (Fig. 5*E*), suggesting defects in the ability of IL-10$^+$ B cells to present BDC2.5 self-peptide to BDC2.5-transgenic CD4$^+$ T cells. Ab-mediated blockade of IL-10 did not alter B-cell Ag-presenting function as determined indirectly via assessment of IFN-γ production by cocultured T cells (Fig. 5*F*). To test whether secretion of the immunoregulatory cytokine IL-10 by Bregs may have a direct effect on activation and/or differentiation of T-effector cells, flow cytometric analysis was performed on CD4$^+$ T cells that were cocultured in the presence of anti–IL-10 blocking or control Ab. Ab-mediated blockade of IL-10 did not significantly affect activation of CD44$^+$CD62L$^-$ T-effector cells or IL-2 and IL-17 production by CD4$^+$ T cells in Breg cocultures but did result in a significant ($P \leq 0.01$) reduction of IL-4 production by CD4$^+$ T cells (Fig. 5*G*).

IL-10$^+$ B Cells From Nglc NOD Mice Exhibit Regulatory Functions Ex Vivo and In Vivo

To study the immunoregulatory properties of naturally occurring IL-10–producing B cells ex vivo, splenic IL-10$^+$ B cells were isolated from Nglc NOD mice and cocultured with CD11c$^+$ DCs and BDC2.5 transgenic CD4$^+$ T cells in the presence of BDC2.5 peptide. IFN-γ production by transgenic CD4$^+$ T cells was significantly ($P \leq 0.05$) decreased in cocultures with IL-10$^+$B220$^+$ B cells compared with IL-10$^-$B220$^+$ B cells (Fig. 5*H*). To test whether IL-10$^+$ B-cell subsets are able to suppress T-cell–mediated destruction of pancreatic islets in vivo, splenic IL-10$^+$ B cells and IL-10$^-$ B-cell subsets were isolated from Nglc NOD mice and adoptively cotransferred with diabetogenic CD4$^+$ T cells into NOD.Scid recipient mice. Consistent with our ex vivo findings, IL-10$^+$B220$^+$ cells suppressed T cell–mediated autoimmune destruction of pancreatic islets and maintained normoglycemia in NOD.Scid mice significantly ($P \leq 0.05$) longer compared with transferred IL-10$^-$ B cells (time free from diabetes: IL-10$^+$ B cells: 15 weeks vs. IL-10$^-$ B cells: 7 weeks post-adoptive transfer; n = 4 mice, respectively) (Fig. 5*I*).

Depletion of Endogenous B Cells, Followed by Adoptive Transfer of B Cells from Hglc NOD Mice, Converts Lnglc hCD20 Transgenic NOD Mice to Hyperglycemia

To show that B cells are at least partially responsible for maintaining normoglycemia in Lnglc NOD mice, we attempted to deplete naïve B cells using an anti-mouse

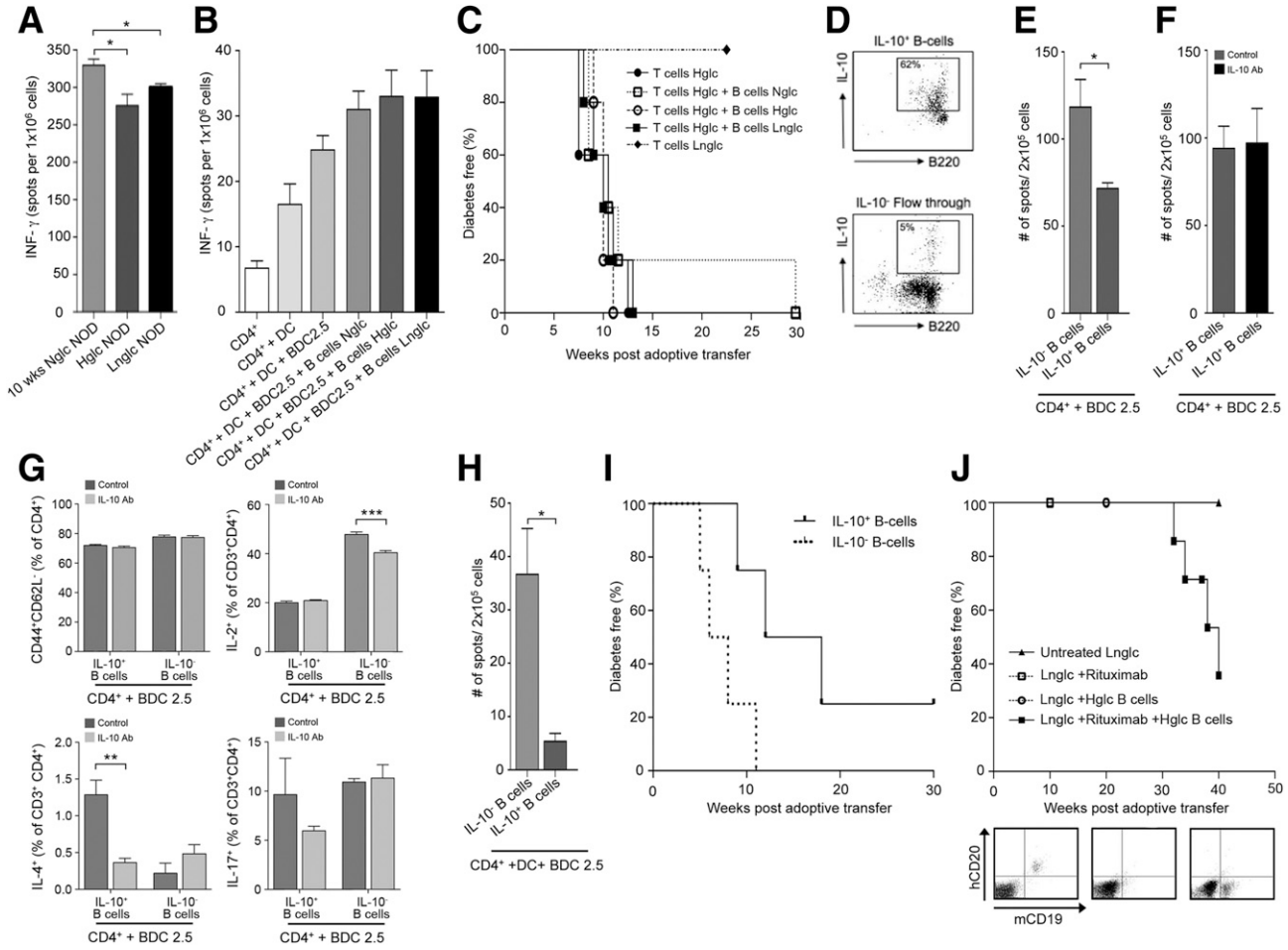

Figure 5—Antigen-presenting and immunoregulatory functions of B-cell populations in NOD mice. *A*: Quantification of IFN-γ–producing cells in an ex vivo ELISPOT assay of $CD4^+$ T cells stimulated by the self-peptide BDC2.5 in the presence of total B cells to assess their Ag-presenting capacities. *B*: Quantification of IFN-γ–producing cells in an ex vivo ELISPOT assay of $CD4^+$ T cells stimulated by BDC2.5 peptide in the presence of bone marrow–derived DCs to assess the immunosuppressive capacity of total B cells isolated from different experimental groups of NOD mice. *C*: Evaluation of diabetes onset after adoptive transfer of B and T cells isolated from Nglc, Hglc, and Lnglc NOD mice into NOD.Scid recipients (n = 5). Kaplan-Meier analysis was used to graph diabetes onset. *D*: Flow cytometry of IL-10^+B220^+ B cells pre- (bottom) and post- (top) enrichment. *E*: Quantification of IFN-γ–producing cells in an ex vivo ELISPOT assay of $CD4^+$ T cells stimulated by BDC2.5 peptide in the presence of IL-10^- or IL-10^+ $B220^+$ B cells and in the presence of anti–IL-10 Ab-mediated blockade (*F*) to assess the immunosuppressive capacity of IL-10^+ vis-à-vis IL-10^- $B220^+$ B cells. *G*: Flow cytometric analysis of T-cell activation (CD44/CD62L) and differentiation (IL-2, -4, and -17 cytokine production) upon Breg coculture. *H*: Quantification of IFN-γ–producing cells in an ex vivo ELISPOT assay of $CD4^+$ T cells stimulated by BDC2.5 peptide in the presence of bone marrow–derived DCs and IL-10^- or IL-10^+ $B220^+$ B cells to assess the immunosuppressive capacity of IL-10^+ vis-à-vis IL-10^- $B220^+$ B cells. *I:* Adoptive co-transfer of IL-10^+B220^+ or IL-10^-B220^+ cells with diabetogenic $CD4^+$ T cells obtained from Hglc NOD mice into NOD.Scid mice (n = 4). Kaplan-Meier analysis was used to graph diabetes onset. *J*: Representative flow cytometry of peripheral B cells in hCD20($^{+/+}$) NOD mice pre–B-cell depletion using rituximab (left), postdepletion (middle), and after adoptive transfer with murine Hglc $CD19^+$ B cells (right), and evaluation of diabetes onset in untreated, rituximab-depleted, and untreated or rituximab-depleted mice that were adoptively transferred with B cells obtained from Hglc NOD mice in Lnglc hCD20($^{+/+}$) NOD mice (n = 3–7, respectively). Kaplan-Meier analysis was used to graph diabetes onset. Bars represent mean ± SEM. wks, weeks. *$P \leq 0.05$; **$P \leq 0.01$; ***$P \leq 0.001$.

CD20-depleting mAb (47). However, consistent with published data (48), flow cytometric analysis revealed a down-regulation of CD20 within the peripheral B-cell pool of Lnglc NOD mice even before injection with the anti-mouse CD20-depleting Ab (data not shown), thus rendering Lnglc NOD mice resistant to B-cell depletion. We therefore used hCD20($^{+/+}$) NOD mice (15) in which B cells are engineered to stably express high levels of human CD20 and are hence susceptible to B-cell depletion with rituximab (anti-human CD20 mAb). Similar to wild-type NOD mice, approximately 10–15% of these animals fail to develop hyperglycemia. We successfully depleted the B-cell compartment of Lnglc hCD20($^{+/+}$) NOD mice and adoptively transferred B cells isolated from Hglc NOD mice 1 week after depletion (Fig. 5*J*). Although 100% of untreated control mice (n = 5), mice depleted with rituximab that did not receive adoptively transferred B cells (n = 4), and mice that were not depleted but received

B cells from Hglc NOD mice (n = 3) maintained normoglycemia for >10 weeks, five of seven B-cell–depleted mice that subsequently received B cells from Hglc NOD mice (n = 7) became hyperglycemic ($P \leq 0.05$) (Fig. 5*J*).

Reduced Frequencies of CD40$^+$ and IL-10$^+$ B Cells Are Observed in Individuals With T1D

To test whether our findings in the NOD mouse model of autoimmune diabetes extend to the human setting, we studied the phenotype of B cells in the peripheral blood of healthy volunteers, individuals with T1D, and relatives of T1D patients with detectable serum levels of aAb but without overt disease. Interestingly, frequencies of CD40$^+$ B cells (Fig. 6*A*), but not CD80$^+$ or MHC class II$^+$ B cells (Fig. 6*B* and *C*), were significantly ($P \leq 0.05$) higher in the peripheral blood of healthy individuals and relatives with serum aAb compared with T1D patients. On contrary, percentages of anergic IgD$^+$IgM$^-$CD27$^-$ B cells (as previously described [49]) were markedly ($P \leq 0.05$) lower in healthy individuals compared with individuals with T1D (Fig. 6*D*). Importantly, IL-10$^+$ B cells were significantly ($P \leq 0.05$) higher in the peripheral blood of healthy individuals compared with relatives with aAb and individuals with T1D (Fig. 6*E*).

Peripheral B Cells From Individuals With T1D Do Not Display Immunoregulatory Properties

To study whether unseparated peripheral B cell populations isolated from healthy individuals or those with T1D possess immunoregulatory functions ex vivo, PBMCs containing or depleted of B cells were cultured in the presence of the islet-specific peptides GAD or IA-2, and IFN-γ–production was quantified. Interestingly, compared with B-cell–depleted PBMC cocultures, stimulation of B-cell–containing PBMCs isolated from T1D patients with IA-2, but not with GAD, resulted in significantly ($P \leq 0.001$) increased levels of IFN-γ production (Fig. 7*B* and *C*), suggesting that whole B-cell subsets have stimulatory but not immunoregulatory activity. T-cell activation in response to Pediacel served as a positive control ($P \leq 0.05$) (Fig. 7*A*).

Individuals With T1D Show Defects in Generating Bregs Ex Vivo

To assess whether individuals with T1D showed defects in Breg generation, peripheral B cells were isolated from healthy control subjects, individuals with T1D, and those with aAb but without T1D and subjected to an ex vivo Breg generation assay. Frequencies of IL-10$^+$ B cells generated from healthy individuals were significantly ($P \leq 0.05$) higher compared with individuals with T1D and aAb$^+$ relatives (Fig. 7*D*).

IL-10$^+$ B Cells From Individuals With T1D Suppress Autoimmune Responses Ex Vivo

To study the immunoregulatory properties of IL-10–producing B cells, IL-10$^+$ B cells were isolated from PBMCs of individuals with T1D, expanded ex vivo, and cocultured with matched PBMCs in the presence of IA-2 peptide. Paralleling our findings in the NOD mouse model, IFN-γ production by T cells was significantly ($P \leq 0.05$) decreased when IL-10$^+$CD19$^+$ B cells, but not IL-10$^-$CD19$^+$ B cells, were added to the coculture (Fig. 7*E*). Pediacel served as a positive control for T-cell activation.

DISCUSSION

Our current understanding of T1D pathogenesis suggests that B cells play a pivotal role in promoting disease onset and progression, yet little is known about their ability to inhibit the autoimmune destruction of pancreatic islets (1–3). Here, we show that a subset of IL-10–producing, immunoregulatory B cells plays a key role in maintaining normoglycemia in a group of NOD mice that were naturally protected from overt disease (i.e., hyperglycemia) and potentially healthy individuals. Conversely, Hglc NOD mice, individuals with established T1D, and individuals with aAbs but without disease demonstrated reduced frequencies of this population of Bregs.

Specifically, we demonstrated that the pancreatic islets of Lnglc NOD mice that are naturally protected from autoimmune diabetes for as-of-yet unknown reasons contained a limited B-cell infiltrate. Surprisingly, IgV_H transcriptome analysis revealed a highly mutated, class-switched B-cell receptor repertoire within islets of Hglc and, to an even greater extent, Lnglc NOD mice, suggestive of an Ag-experienced B-cell pool. Further examination of the VDJ junction within IgV_H transcripts revealed a progressive increase in clonal diversity within islet-infiltrating B cells from 4-week-old Nglc to Hglc NOD mice, suggesting that the B-cell repertoire continues to undergo affinity maturation (44,45) during the manifestation of diabetes. In contrast, we observed fewer individual clones within islets of Lnglc mice. In summary, we identified hallmark features of affinity maturation, namely somatic hypermutation, insertions and deletions, and isotype switching (44,45) in Hglc and, to an even greater extent, Lnglc NOD mice. We therefore propose that islets from Lnglc NOD mice are infiltrated by a pool of highly matured, selected B-cell clones with a unique specificity against islet-associated antigens, whereas lower-affinity clones were previously removed by negative selection. This hypothesis is supported by our findings of increased frequencies of apoptotic and anergic B cells within the pancreatic islets of Lnglc mice.

Although the age difference between Hglc (~19 weeks) and Lnglc (~30 weeks) mice may allow for B cells to acquire receptor diversity by incorporating stochastic mutations over time, data showing the accumulation of mutations specifically within the CDR3 region suggests that the pancreatic islets provide a distinct microenvironment in which B cells, upon Ag encounter, can undergo affinity maturation and clonal expansion. Importantly, islet-infiltrating B cells from Lnglc NOD mice proved to be highly mature and clonally expanded without promoting autoimmune destruction of insulin-producing β-cells, indicating that these B cells are functionally impaired

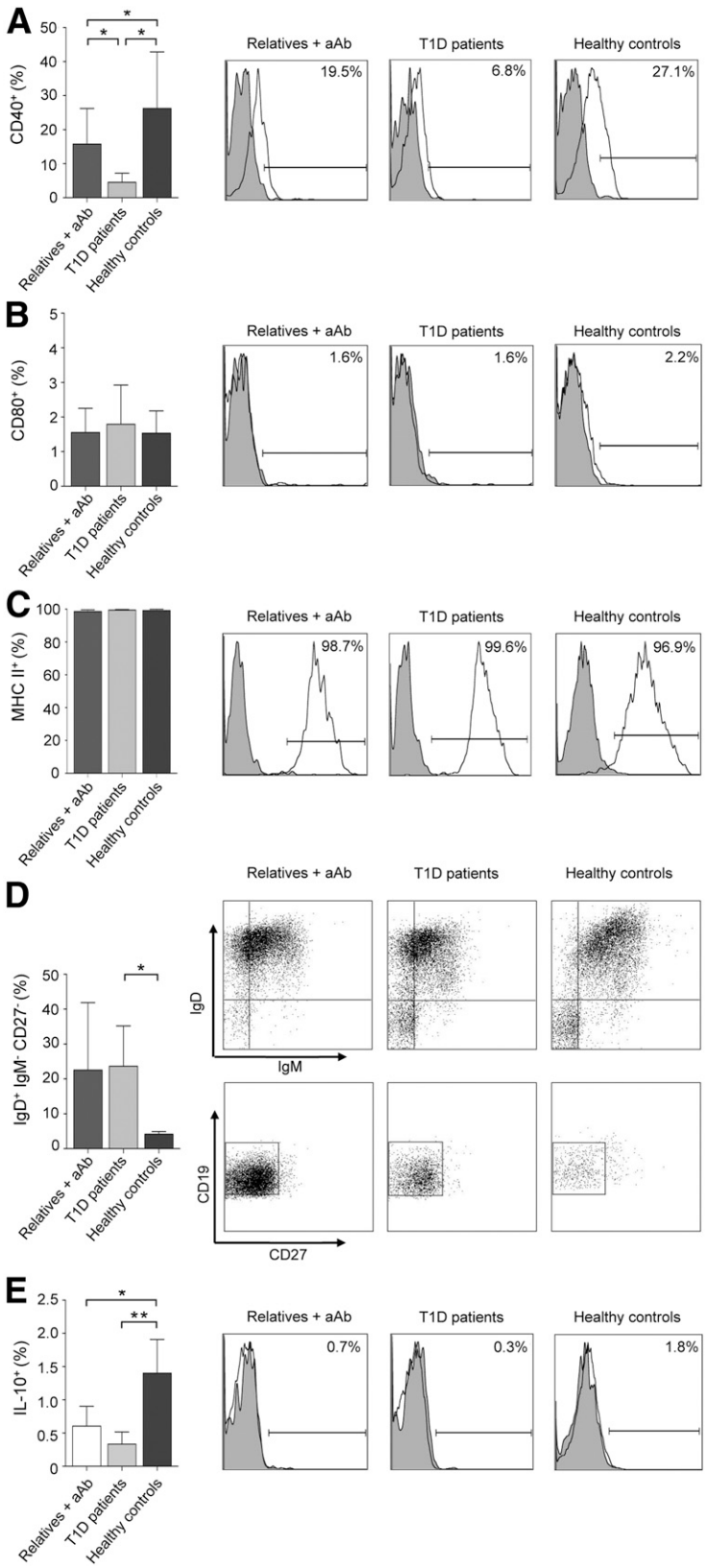

Figure 6—Phenotypic characterization of human peripheral B cells. Expression of the B-cell activation markers CD40 (*A*), CD80 (*B*), and MHC II (*C*) by $CD19^+$ B cells isolated from PBMCs of healthy individuals, aAb^+ relatives, and individuals with T1D. Frequencies of anergic $IgD^+IgM^-CD27^-CD19^+$ B cells (*D*) and of IL-10^+ $CD19^+$ B cells (*E*) isolated from PBMCs of healthy individuals, aAb^+ relatives, and individuals with T1D as determined by flow cytometry. White peaks indicate antigen-specific staining, gray peaks show respective isotype control staining. Mean percentages of marker expression (left) and representative flow cytometric plots (right). Bars represent mean ± SEM.*$P \leq 0.05$; **$P \leq 0.01$.

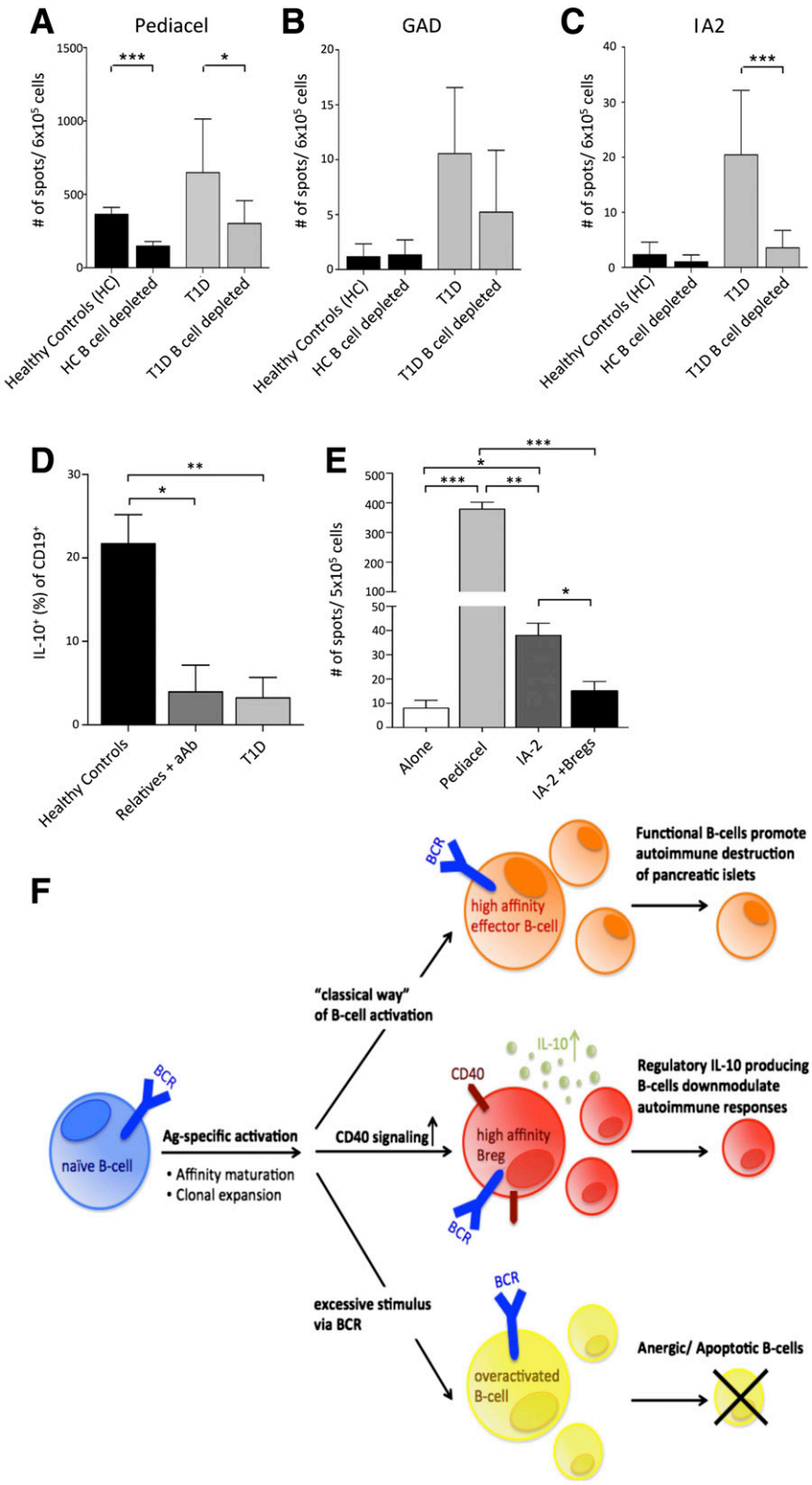

Figure 7—Immunoregulatory properties of human B cells. *A*: Quantification of IFN-γ–producing cells within PBMCs or B-cell–depleted PBMCs stimulated ex vivo with Pediacel (positive control) (*A*) or the aAgs GAD (*B*) and IA-2 (*C*), as determined by ELISPOT assay. *D*: Quantification of ex vivo–generated IL-10$^+$CD19$^+$ B cells, as determined by flow cytometry. *E*: Quantification of IFN-γ–producing cells within PBMCs isolated from T1D patients stimulated ex vivo with IA-2 in the presence or absence of IL-10$^+$CD19$^+$ B cells, as determined by ELISPOT assay. *F*: Hypothesis summarizing the generation of autoreactive, anergic, or Bregs in the context of autoimmunity. Bars represent mean ± SEM. *$P \leq 0.05$; **$P \leq 0.01$; ***$P \leq 0.001$.

and/or able to negatively regulate autoimmunity. Islets from Lnglc mice maintained high frequencies of both $CD40^+$ and IL-10^+ B cells compared with 10-week-old Nglc or Hglc NOD mice. Likewise, healthy individuals and aAb-positive relatives of T1D patients exhibit increased frequencies of $CD40^+$ and IL-10^+ B cells when compared to individuals with T1D. It has been previously shown that CD40 signaling induces IL-10 competence in B cells (50,51). In addition IL-10 has been described to exert anti-inflammatory effects, while enhancing survival, proliferation, differentiation, and isotype switching of B cells (52). Increased CD40 signaling in Lnglc NOD mice, healthy individuals, and relatives with serum aAb may possibly provide a strong stimulus, which could induce anergy or apoptosis in these hyperactivated B cells (14) or stimulate the generation of Bregs (50,51). Phenotypic analysis of B-cell populations in the periphery revealed differences between B-cell subsets in the blood of healthy individuals versus T1D patients, while no significant differences were observed between splenic B cells from normoglycemic versus hyperglycemic NOD mice. This may, at least in part, be due to the fact that the disease persists much longer in humans compared to mice, thus allowing sufficient numbers of B cells to migrate from the pancreatic microenvironment, where they are imprinted, to the periphery.

Our data further suggest that IL-10 plays a pivotal role in mediating immunosuppressive functions, as only IL-10^+ B cells, but not whole B-cell populations or IL-10^- B-cell subsets, were able to suppress autoreactive T-cell activation ex vivo and prevent diabetes onset in vivo. Importantly, rituximab-mediated depletion of B cells followed by adoptive transfer of B cells from Hglc NOD mice converted Lnglc hCD20($^+/^+$) NOD mice to hyperglycemia. Finally, the observed defect in generation of IL-10^+ B cells in patients with T1D compared to healthy individuals further suggests that the tolerance mechanism we identified in the experimental NOD mouse model may, at least in part, translate to human disease.

Together, our findings provide novel insights on a population of naturally occurring, highly matured Breg that mediate protection against autoimmune destruction of pancreatic islets and possess the potential requirements for maintenance and expansion in vivo (Fig. 7*F*). Our data further suggest that in the setting of T1D, the inflammatory microenvironment renders this B-cell subset functionally impaired or apoptotic. This novel population of B cells may hold the potential to restore tolerance to aAg in individuals with T1D, which remains a major challenge for investigators in the field.

Funding. P.F. received a JDRF Career Development Award, an American Society of Nephrology Career Development Award, an American Diabetes Association (ADA) Mentor-based Fellowship grant, and is supported by an American Heart Association (AHA) Grant-In-Aid, Translational Research Program (TRP) grant from Boston Children's Hospital, and Harvard Stem Cell Institute grant ("Diabetes Program" DP-0123-12-00). P.F. also received Italian Ministry of Health grants RF-2010-2303119 and "Staminali" RF-FSR-2008-1213704. A.V. has been supported by a National Institutes of Health (NIH) Research Training grant to Boston Children's Hospital in Pediatric Nephrology (T32-DK-007726-28). M.B.N. is supported by an ADA Mentor-based Fellowship grant to P.F. R.B. is supported by an American Society of Transplantation/Genentech Clinical Science Fellowship grant. L.W. is supported by JDRF (4-2007-1059) and NIH (RC1DK087699 and DK088181).

Duality of Interest. No potential conflicts of interest relevant to this article were reported.

Author Contributions. S.K., A.V., and P.F. planned the project. S.K., A.V., S.T., M.B.N., M.A.N., S.W., and R.B. carried out experimental work. S.K., A.V., S.T., M.B.N., M.A.N., S.W., R.B., F.D., T.S., R.A., M.A., M.H.S., L.W., C.H.W., K.C.O., and P.F. analyzed data. S.K. and P.F. wrote the manuscript. All authors discussed the results and commented on the manuscript. P.F. is the guarantor of this work and, as such, had full access to all the data in the study and takes responsibility for the integrity of the data and the accuracy of the data analysis.

References

1. Bluestone JA, Pardoll D, Sharrow SO, Fowlkes BJ. Characterization of murine thymocytes with CD3-associated T-cell receptor structures. Nature 1987; 326:82–84

2. Noorchashm H, Noorchashm N, Kern J, Rostami SY, Barker CF, Naji A. B-cells are required for the initiation of insulitis and sialitis in nonobese diabetic mice. Diabetes 1997;46:941–946

3. Fiorina P, Vergani A, Dada S, et al. Targeting CD22 reprograms B-cells and reverses autoimmune diabetes. Diabetes 2008;57:3013–3024

4. Serreze DV, Chapman HD, Varnum DS, et al. B lymphocytes are essential for the initiation of T cell-mediated autoimmune diabetes: analysis of a new "speed congenic" stock of NOD.Ig mu null mice. J Exp Med 1996;184:2049–2053

5. Lanzavecchia A. Antigen-specific interaction between T and B cells. Nature 1985;314:537–539

6. Silveira PA, Dombrowsky J, Johnson E, Chapman HD, Nemazee D, Serreze DV. B cell selection defects underlie the development of diabetogenic APCs in nonobese diabetic mice. J Immunol 2004;172:5086–5094

7. Wong FS, Wen L, Tang M, et al. Investigation of the role of B-cells in type 1 diabetes in the NOD mouse. Diabetes 2004;53:2581–2587

8. Falcone M, Lee J, Patstone G, Yeung B, Sarvetnick N. B lymphocytes are crucial antigen-presenting cells in the pathogenic autoimmune response to GAD65 antigen in nonobese diabetic mice. J Immunol 1998;161:1163–1168

9. Marino E, Batten M, Groom J, et al. Marginal-zone B-cells of nonobese diabetic mice expand with diabetes onset, invade the pancreatic lymph nodes, and present autoantigen to diabetogenic T-cells. Diabetes 2008;57:395–404

10. Serreze DV, Fleming SA, Chapman HD, Richard SD, Leiter EH, Tisch RM. B lymphocytes are critical antigen-presenting cells for the initiation of T cell-mediated autoimmune diabetes in nonobese diabetic mice. J Immunol 1998;161: 3912–3918

11. Greeley SA, Katsumata M, Yu L, et al. Elimination of maternally transmitted autoantibodies prevents diabetes in nonobese diabetic mice. Nat Med 2002;8: 399–402

12. Inoue Y, Kaifu T, Sugahara-Tobinai A, Nakamura A, Miyazaki J, Takai T. Activating Fc gamma receptors participate in the development of autoimmune diabetes in NOD mice. J Immunol 2007;179:764–774

13. Lund FE. Cytokine-producing B lymphocytes-key regulators of immunity. Curr Opin Immunol 2008;20:332–338

14. Mauri C, Bosma A. Immune regulatory function of B cells. Annu Rev Immunol 2012;30:221–241

15. Hu CY, Rodriguez-Pinto D, Du W, et al. Treatment with CD20-specific antibody prevents and reverses autoimmune diabetes in mice. J Clin Invest 2007; 117:3857–3867

16. Zekavat G, Rostami SY, Badkerhanian A, et al. In vivo BLyS/BAFF neutralization ameliorates islet-directed autoimmunity in nonobese diabetic mice. J Immunol 2008;181:8133–8144

17. Xiu Y, Wong CP, Bouaziz JD, et al. B lymphocyte depletion by CD20 monoclonal antibody prevents diabetes in nonobese diabetic mice despite isotype-specific differences in Fc gamma R effector functions. J Immunol 2008;180:2863–2875
18. Fiorina P, Sayegh MH. B cell-targeted therapies in autoimmunity: rationale and progress. F1000 Biol Rep 2009;1:39
19. Pescovitz MD, Greenbaum CJ, Krause-Steinrauf H, et al. Rituximab, B-lymphocyte depletion, and preservation of beta-cell function. N Engl J Med 2009; 361:2143–2152
20. Mauri C. Regulation of immunity and autoimmunity by B cells. Curr Opin Immunol 2010;22:761–767
21. Iwata Y, Matsushita T, Horikawa M, et al. Characterization of a rare IL-10-competent B-cell subset in humans that parallels mouse regulatory B10 cells. Blood 2011;117:530–541
22. Yanaba K, Bouaziz JD, Haas KM, Poe JC, Fujimoto M, Tedder TF. A regulatory B cell subset with a unique CD1dhiCD5+ phenotype controls T cell-dependent inflammatory responses. Immunity 2008;28:639–650
23. Matsushita T, Yanaba K, Bouaziz JD, Fujimoto M, Tedder TF. Regulatory B cells inhibit EAE initiation in mice while other B cells promote disease progression. J Clin Invest 2008;118:3420–3430
24. Yoshizaki A, Miyagaki T, DiLillo DJ, et al. Regulatory B cells control T-cell autoimmunity through IL-21-dependent cognate interactions. Nature 2012;491: 264–268
25. Blair PA, Chavez-Rueda KA, Evans JG, et al. Selective targeting of B cells with agonistic anti-CD40 is an efficacious strategy for the generation of induced regulatory T2-like B cells and for the suppression of lupus in MRL/lpr mice. J Immunol 2009;182:3492–3502
26. DiLillo DJ, Matsushita T, Tedder TF. B10 cells and regulatory B cells balance immune responses during inflammation, autoimmunity, and cancer. Ann N Y Acad Sci 2010;1183:38–57
27. Watanabe R, Ishiura N, Nakashima H, et al. Regulatory B cells (B10 cells) have a suppressive role in murine lupus: CD19 and B10 cell deficiency exacerbates systemic autoimmunity. J Immunol 2010;184:4801–4809
28. Lin W, Cerny D, Chua E, et al. Human Regulatory B Cells Combine Phenotypic and Genetic Hallmarks with a Distinct Differentiation Fate. J Immunol 2014;193:2258–2266
29. Yanaba K, Bouaziz JD, Matsushita T, Tsubata T, Tedder TF. The development and function of regulatory B cells expressing IL-10 (B10 cells) requires antigen receptor diversity and TLR signals. J Immunol 2009;182:7459–7472
30. Evans JG, Chavez-Rueda KA, Eddaoudi A, et al. Novel suppressive function of transitional 2 B cells in experimental arthritis. J Immunol 2007;178:7868–7878
31. Mauri C, Gray D, Mushtaq N, Londei M. Prevention of arthritis by interleukin 10-producing B cells. J Exp Med 2003;197:489–501
32. Lenert P, Brummel R, Field EH, Ashman RF. TLR-9 activation of marginal zone B cells in lupus mice regulates immunity through increased IL-10 production. J Clin Immunol 2005;25:29–40
33. Ding Q, Yeung M, Camirand G, et al. Regulatory B cells are identified by expression of TIM-1 and can be induced through TIM-1 ligation to promote tolerance in mice. J Clin Invest 2011;121:3645–3656
34. Blair PA, Norena LY, Flores-Borja F, et al. CD19(+)CD24(hi)CD38(hi) B cells exhibit regulatory capacity in healthy individuals but are functionally impaired in systemic lupus erythematosus patients. Immunity 2010;32:129–140
35. Mauri C, Ehrenstein MR. The 'short' history of regulatory B cells. Trends Immunol 2008;29:34–40
36. Bouaziz JD, Yanaba K, Tedder TF. Regulatory B cells as inhibitors of immune responses and inflammation. Immunol Rev 2008;224:201–214
37. Fillatreau S, Sweenie CH, McGeachy MJ, Gray D, Anderton SM. B cells regulate autoimmunity by provision of IL-10. Nat Immunol 2002;3:944–950
38. Correale J, Farez M, Razzitte G. Helminth infections associated with multiple sclerosis induce regulatory B cells. Ann Neurol 2008;64:187–199
39. Anderson MS, Bluestone JA. The NOD mouse: a model of immune dysregulation. Annu Rev Immunol 2005;23:447–485
40. Andre I, Gonzalez A, Wang B, Katz J, Benoist C, Mathis D. Checkpoints in the progression of autoimmune disease: lessons from diabetes models. Proc Natl Acad Sci USA 1996;93:2260–2263
41. Goudy KS, Burkhardt BR, Wasserfall C, et al. Systemic overexpression of IL-10 induces CD4+CD25+ cell populations in vivo and ameliorates type 1 diabetes in nonobese diabetic mice in a dose-dependent fashion. J Immunol 2003;171: 2270–2278
42. Ansari MJ, Fiorina P, Dada S, et al. Role of ICOS pathway in autoimmune and alloimmune responses in NOD mice. Clin Immunol 2008;126:140–147
43. Carvello M, Petrelli A, Vergani A, et al. Inotuzumab ozogamicin murine analog-mediated B-cell depletion reduces anti-islet allo- and autoimmune responses. Diabetes 2012;61:155–165
44. Willis SN, Mallozzi SS, Rodig SJ, et al. The microenvironment of germ cell tumors harbors a prominent antigen-driven humoral response. J Immunol 2009; 182:3310–3317
45. Bradshaw EM, Orihuela A, McArdel SL, et al. A local antigen-driven humoral response is present in the inflammatory myopathies. J Immunol 2007;178:547–556
46. Merrell KT, Benschop RJ, Gauld SB, et al. Identification of anergic B cells within a wild-type repertoire. Immunity 2006;25:953–962
47. Hu C, Deng S, Wong FS, Wen L. Anti-CD20 treatment prolongs syngeneic islet graft survival and delays the onset of recurrent autoimmune diabetes. Ann N Y Acad Sci 2008;1150:217–219
48. Serreze DV, Chapman HD, Niens M, et al. Loss of intra-islet CD20 expression may complicate efficacy of B-cell-directed type 1 diabetes therapies. Diabetes 2011;60:2914–2921
49. Habib T, Funk A, Rieck M, et al. Altered B cell homeostasis is associated with type I diabetes and carriers of the PTPN22 allelic variant. J Immunol 2012; 188:487–496
50. Poe JC, Smith SH, Haas KM, et al. Amplified B lymphocyte CD40 signaling drives regulatory B10 cell expansion in mice. PLoS One 2011;6:e22464
51. Bishop GA, Hostager BS. Signaling by CD40 and its mimics in B cell activation. Immunol Res 2001;24:97–109
52. Moore KW, de Waal Malefyt R, Coffman RL, O'Garra A. Interleukin-10 and the interleukin-10 receptor. Annu Rev Immunol 2001;19:683–765